Indian Journal of Pure & Applied Physics
Vol. 55, May 2017, pp. 363-367

Performance of silicon micro ring modulator with an interleaved *p-n* junction for optical interconnects

Priyanka Goyal* & Gurjit Kaur

School of Information and Communication Technology, Gautam Buddha University, Greater Noida 201 308, India

Received 2 November 2016; revised 27 January 2017; accepted 6 February 2017

Silicon micro ring modulators are critical components in optical on-chip communications. The performance of an interleaved *p-n* junction micro ring modulator using FDTD solutions has been characterized. In this paper, the model and simulation of a modulator utilizing an interleaved junction with a SiO_2layer with a thickness of 10 µm have been presented. It is demonstrated that a loss of 34.7 dB/cm occurs during transmission. The modulator operates at 1.55 µm wavelength with a $V\pi L$ of 0.78 V-cm at a voltage of 1 V, which gives figure of merit.

Keywords: Silicon photonics, Modulators, Interleaved junction, Mach-Zehnder modulators

1 Introduction

Photonic integrated circuit (PIC) is a revolutionary technology because unlike electronic circuits which use electrons as its data carrier, it uses photons as data carriers. Photons are quanta of light which has much more speed of travel than electronic currents. This gives PIC technology a large transfer rate. Several analyses have been carried out in the field of Si photonics[1] because of its immense applications in optical interconnects[2] and conjointly its compatibility with the complementary metal oxide semiconductor (CMOS) technology. Generally, restraining the modulator losses plays a crucial role in gathering the rigorous link budget necessities of data communicationideas. Higher doping levels inside the silicon substance conductor usually results in lower figure of merit, i.e., $V\pi L$, and consequently minimum driving voltages. However, this certainly convinces higher losses, making an elementary altercation inside the design of cost-effective modulators. As an example, the planning of Mach-Zehnder modulator is that each one ought to expertise the whole length of fixed conductor, inevitably resulting in higher losses[3,4]. To minimize the losses, either the doping level or the active length would need to be diminished. This leads to either an enhancement of the requirements of the drive voltages (power consumption) or a decrease in loss. In distinction, metal silicon photonic modulators supported a micro-ring resonator vogue that will have little insertion loss, as most light fall at off -resonant level will pass through the entire ring, having small collaboration with the dopants having lossy characteristics. Therefore, doping levels are boosted for the absolute best modulation proficiency and biggest capacitance whereas not having an enormous effect upon the modulator loss. A micro-ring modulator, a product of silicon as the main material along with silicon dioxide as an oxide layer of 10 µm, operating with 1 V pressure voltage, and 1.55 µm wavelength on 193.4 THz simulation frequency has been simulated and analyzed on Lumerical software package.

2 Device Structure

In a micro-ring structure, changes to the effective index of the waveguide will result in a shift in the resonant frequency, which can be used to modulate an optical signal. This change in effective index is driven by modulation of the carrier density in an electrically active waveguide. In the structure, silicon on insulator process is being used where Si thin film of 2 µm is formed epitaxially on silicon oxide layer of 10 µm. Waveguide structures will be patterned after etching of silicon. In the referenced device, interleaved *p-n* junctions are shaped by alternately doping *p*-type and *n*-type hands along the directions of the waveguide. The resulting shape and doping profile have replicate symmetry along the lines inside the center of every doping finger. This is illustrated within the top-down view of the waveguide designed in the Fig. 1.

*Corresponding author (E-mail: pri_2288@yahoo.co.in)

The structure of the micro-ring modulator is designed in accordance with Rosenberg *et al.*[5] The dimensions of the micro-ring modulator and its high doping profile are being used to determine profile of the interleaved *p-n* junction. In Fig. 2, silicon slab of 2 µm is implanted above the silicon oxide substrate of 10 µm with a waveguide of 0.5 µm. Here, in response to 1 V applied voltage across the cathode, electrons and holes have been distributed under electrical simulation. Refractive index changes according to the charge distribution inside the modulator that also changes the refractive index of the optical mode which is determined by the overlapping amongst charge distribution and the profile of optical mode. Total charge inside the modulator is:

$$Q = \int CdV \quad \ldots (1)$$

Power consumption of the modulated data is $\frac{1}{4}\,CV^2$, therefore, both applied voltage and capacitance should be minimized to obtain lower power consumption. When the diode is forward biased the hole densities and electrons in the intrinsic region are equal so that the total charge carried by holes and electrons must satisfy the relation between charge and capacitance. As can be seen, power depends linearly on capacitance.

Capacitance value can be calculated as:

$$C = \frac{Q(V+\Delta V)-Q(V)}{\Delta V} \quad \ldots (2)$$

ΔV is taken to be 0.25 mV at every step. When the stored charges in the junction are removed the junction voltage is calculated by the depletion charge and depletion layer capacitance. Figure 3 shows the effect of voltage on the capacitance. As the voltage at the cathode increases, capacitance of the waveguide decreases. Initially at 0 V its value is 0.87 fF/µm and at 1V it is 0.67 fF/µm.

Figure 4 describes the FDTD solver which uses carrier density to detect effective index across the optical simulation. In order to detect higher phase shifter efficiency, capacitance per unit length should be higher. But as we increase the size of the phase shifter, inductance increases which further lowers overlap factor and eventually velocity of propagation mismatches between optical and electrical simulation. That is why shorter phase shifter is being used.

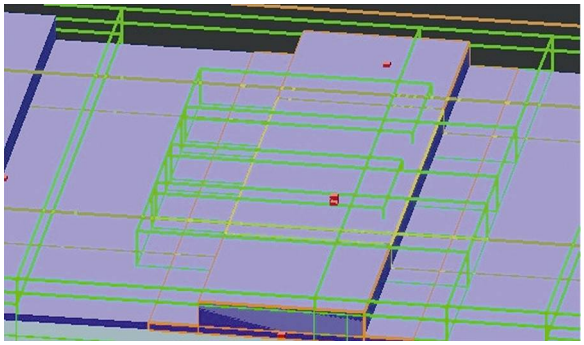

Fig. 1 – Perspective view of the interleaved junction

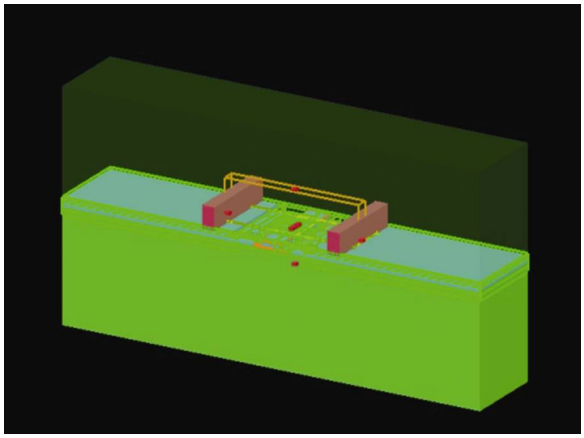

Fig. 2 – Micro-ring modulator 3D view

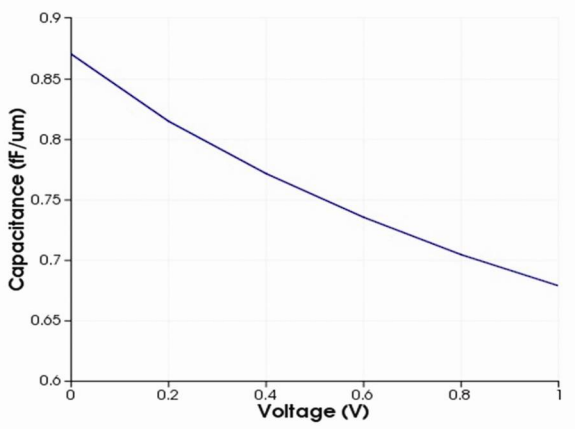

Fig. 3 – Capacitance versus voltage

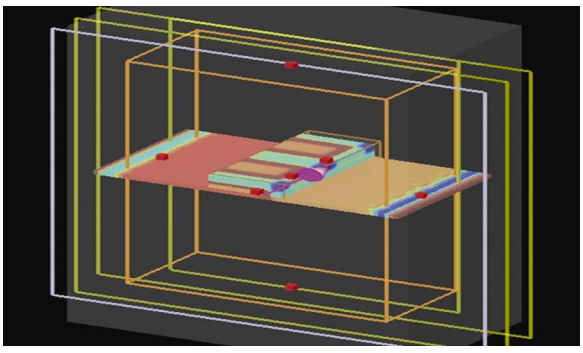

Fig. 4 – Perspective view while optical simulation is being implemented

In interleaved phase shifter, two segments are there which are placed along the length of the waveguide alternatively. As shown in Fig. 5 vertical *p-n* junction is present along with the horizontal *p-n* junction which is present in the second segment. Along the waveguide, vertical *p-n* junction and horizontal *p-n* junction are placed one after another and at interface extra *p-n* junction forms which increases capacitance per length.

3 Simulation and Results

Electrical manipulation in the charge density in interaction with propagation of light can be obtained by various mechanisms such as depletion, accumulation and charge injection. For high speed operation depletion is the most suitable method which can be realized by reverse biased *p-n* junction. Figure 6 describes charge profile over the entire volume of the micro-ring modulator. Across the cathode and anode where voltage is being transferred and charge intensity is low.

In Figs 7 and 8, charge intensity *p* decreases as the applied voltage increases. Same will happen to charge *n* at 0 V and 1 V. However, these electric field effects are weak in case of silicon at 1550 nm wavelength. The thermooptic coefficient for silicon is very high. So, it is not easy to achieve high speed modulation.

From Figs 9-12 it can be concluded that electric field diverges with the increase in the applied voltage. Divergence of electric field appears to be far field type scalar anisotropic field. It can be

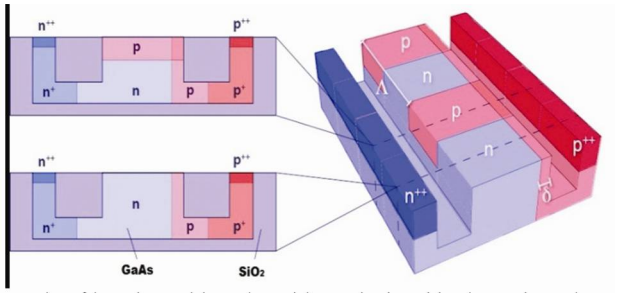

Fig. 5 – Schematic of interleaved junctionwith vertical and horizontal *p-n* junction diodes

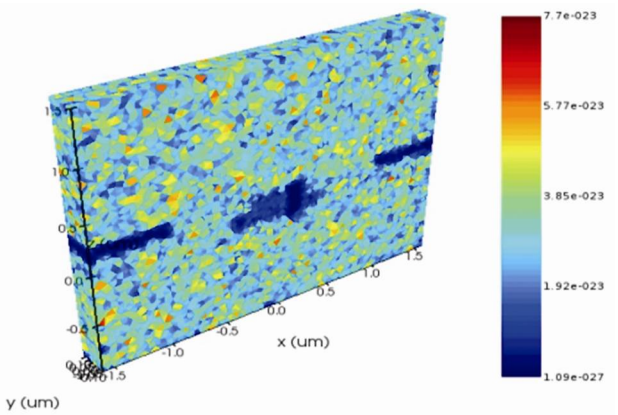

Fig. 6 – Charge distribution in whole structure

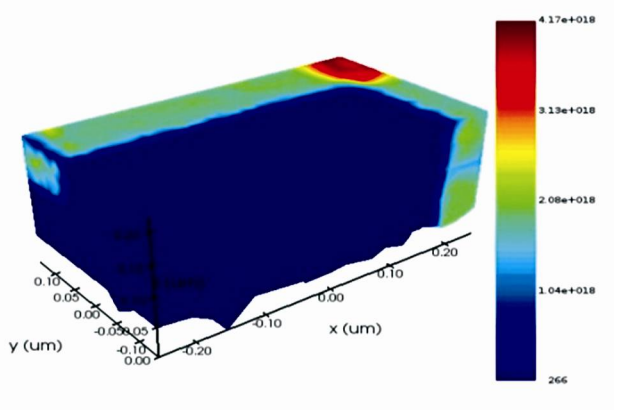

Fig. 7 – Positive charge *p-n* junction at 0V

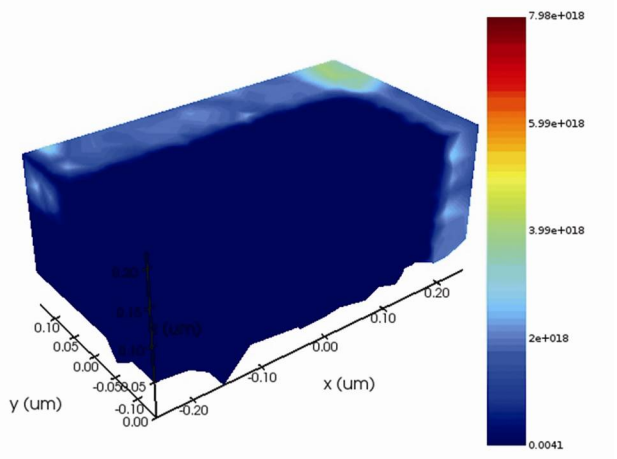

Fig. 8 – Charge *p* at 1 V

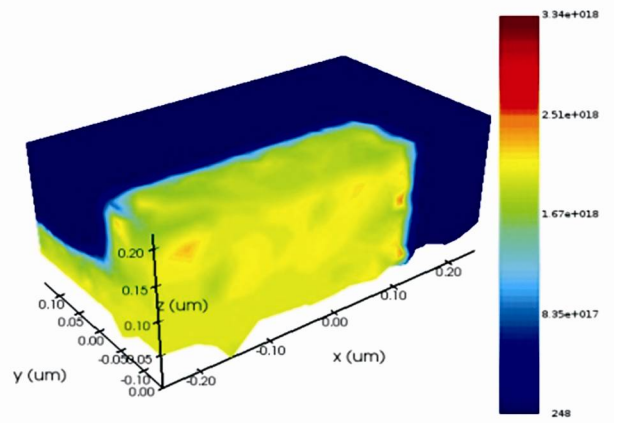

Fig. 9 – Charge and distribution over entire volume at 0 V

generated by time varying current and electric charge. The experimental observation for these results is time varying electric charges or currents should be fast.

For better operation of modulator the four key parameters are insertion loss, modulation efficiency, return loss and response speed. As shown in Fig. 13(a) interleaved junction provides a low $V\pi L$ of 0.78 V-cm. The fundamental mode within the wave guide will be TE mode. Therefore, the *x*-component of the electrical field (*Ex*) at the center of the waveguide is averaged over one amount of the interleaved dopants. The fraction of a full π section shift will then be determined, yielding the complete length needed for a section shift of π radians ($L\pi$):

$$\Delta\varphi(V) = \frac{2\pi}{\lambda_0}\Delta n_{eff}(V)L_\lambda = a\pi \rightarrow L\pi = \frac{L_\lambda}{a} \quad \ldots (3)$$

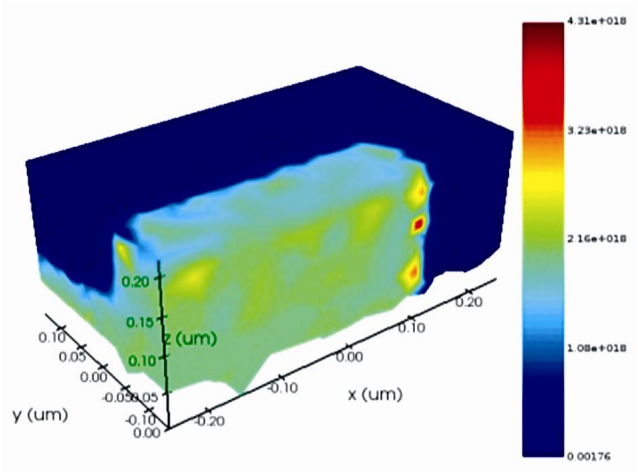

Fig. 10 – Charge and distribution over entire volume at 1 V

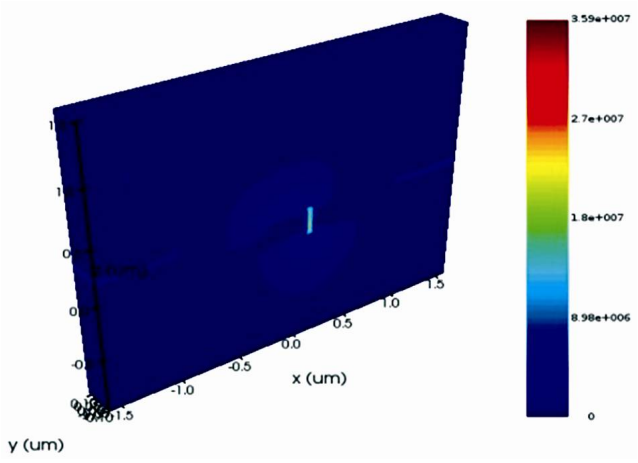

Fig. 11 – Electric field distribution across the structure at 0 V

Figure of merit, i.e., $V\pi L$ is the product of $L\pi$ and its corresponding voltage *V*, i.e., 1 V. The free electrons are accumulated within the thin layer. The variation in the refractive index overlaps with the optical mode is very low which yield low modulation efficiency.

The interleaved *p-n* junction modulator has both *p* type and *n* type segments of equal length. Forward biased PIN diode is widely used to obtain changes in the refractive index by injecting carriers in to lightly doped region of the diode. The periodicity in the modulation refractive index is also maintained. Return loss arising from the Bragg reflection are expected from such structure. Recent work has been focused on the transmission loss in interleaved *p-n* junction modulator. Figure 13(b) shows the loss from the transmission that will be calculated directly, i.e., 34.7 dB/cm. Also, it is normalized to the doping period (500 nm) to obtain values in dB/cm. Figure 13(c) shows the net effective refractive index (n_{eff}) with the voltage *V*. The graph shows that as we increase the voltage of the modulator its refractive index changes accordingly and also its resonant frequency changes which is used to modulate an optical signal. Figure 13(d) describes transmission $T_x$along the wavelength. At 0 μm (*x* direction) the transmission rate is highest and as we go further from 0 μm its intensity faded away. Figure 13(e) shows the electric field profile which is highest at the center, i.e., at 0 μm (at *x*) and it also decreases on both sides as transmission does. From the above results it is concluded that the modulator performance is governed by doping level in the modulator, the various geometrical parameters including the length and width of interleaved segment.

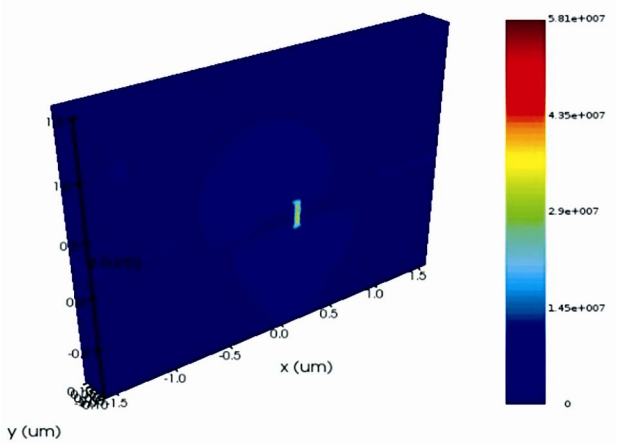

Fig. 12– Electric field distribution across the structure at 1 V

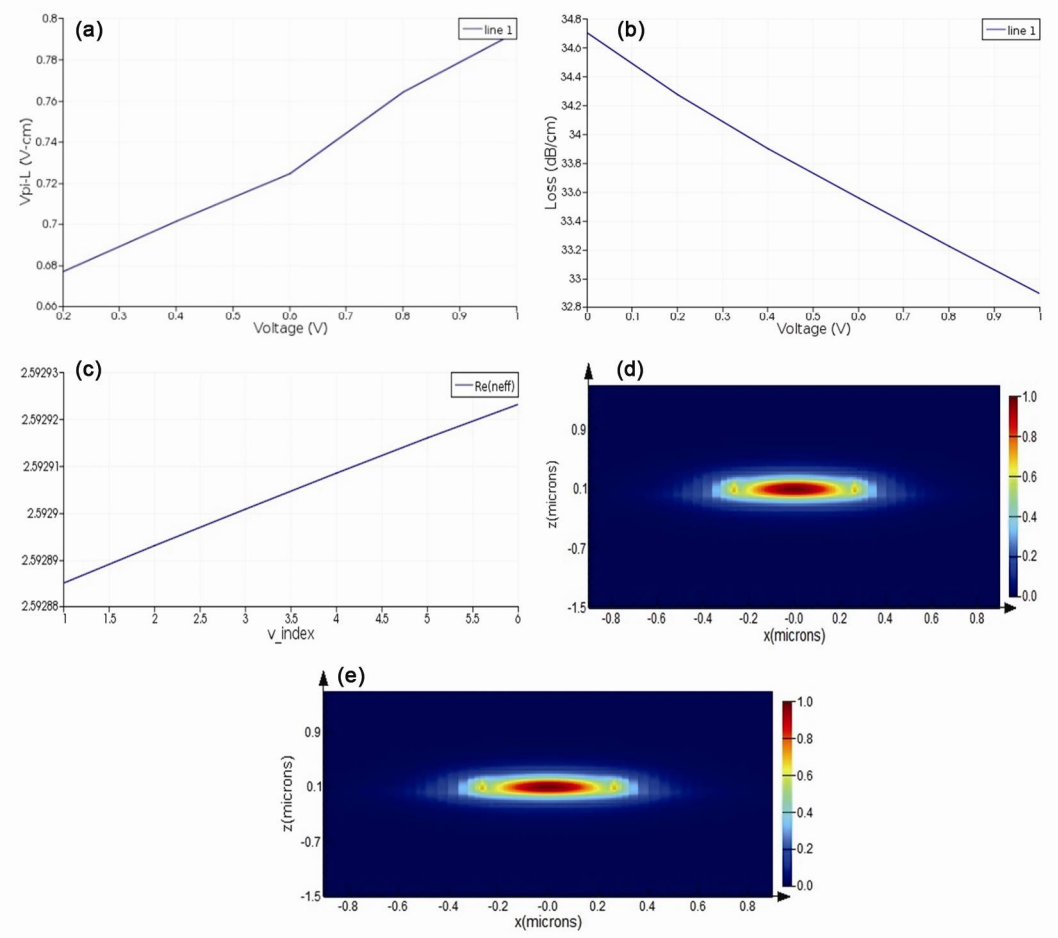

Fig. 13 – (a) $V\pi L$ at 1 V of applied voltage, (b) loss in dB at 1V applied voltage, (c) net effective refractive index (n_{eff}) with the voltage V, (d) transmission $T_x$along the wavelength and (e) electric field profile

4 Conclusions

Silicon electro-optic microring modulator is implemented and simulated with an interleaved *p-n* junction in order to find low figure of merit $V\pi L$ which is found to be 0.78 V-cm and also low loss in dB/cm, whose value is 34.7 dB/cm. Lower VπL values have been found but under higher propagation losses, i.e., up to 75 dB/cm.

References

1 Thomson D J, Gardes F, Fedeli J M & Zlatanovic S, *IEEE Photon Technol Lett*, 24 (2012) 234.

2 Pepeljugoski P, Kash J, Doany F & Kuchta D, *Low power and high density optical interconnects for future supercomputers*,Optical Fiber Communication Conference, 2010.

3 Ding J, Chen H, Yang L & Zhang L, *Opt Express*, 20 (2012) 7081.

4 Watts M R, Zortman W A, Trotter D C, Young R W & Lentine A L,*IEEE J Sel Top Quantum Electron*,16 (2010) 159.

5 Rosenberg J C, Green W M J, Assefa S & Gill D M, *Opt Express*, 20 (2012) 26411.